Research Article

Xi Liu, Ying Li*, Ling Long, Hailong Wang, Qingfeng Guo, Qingchun Wang, Jing Qi, Jia Chen, Yan Long, Ji Liu, and Zuowan Zhou*

Preparation and bonding mechanisms of polymer/metal hybrid composite by nano molding technology

https://doi.org/10.1515/ntrev-2022-0120 received April 7, 2022; accepted May 10, 2022

Abstract: With the development of nano molding technology (NMT), the polymer/metal hybrid (PMH) composites have made great progress in industries like automobile, aircraft, and boat. The bonding structure and bonding strength are the key factors ruling the application of PMH. In this work, the PMH containing polyphenylene sulfide (PPS) and Al alloy was prepared by NMT, and the surface treating of Al alloy and the bonding mechanism of PMH has been studied. The results reveal that the bonding strength between metal and polymer shows dependence on the pore structure of the metal surface, which could be controlled by changing the anodizing voltage and time. The PMH in which the Al plate was anodized at 15 V for 6 h achieves the best bonding strength of 1,543 N. The morphological analysis reveals that there forms an anchor and bolt structure in the interface of PPS and Al plate, which bonds the polymer and metal tightly. In addition, the chemical interaction between PPS and Al was confirmed by attenuated total reflection (ATR) infrared spectroscopy, which indicates that both physical and chemical effects contribute to the bonding strength of the PMH. This PMH has great potential of being used as alternative to traditional pure metal components,

Keywords: nano molding technology, polymer metal hybrids, bonding mechanism

1 Introduction

In recent years, metal resin composite materials, polymer metal hybrids (PMH), fabricated by nano molding technology (NMT) have made great progress in the electronics, automotive, aerospace, and other industries due to their advantages of high strength and lightweight [1-3]. PMH refers to composites in which metal and resin are combined face to face and synchronously generated boundaries where the metal and polymer interpenetrated together [4,5]. For the combination of metal and polymers, it is difficult to bond them together without adhesive or surface treating, and the weak interfacial interaction force between the metal and resin limits the wide application of such composite materials. PMH prepared by NMT saves the cost of adhesive or surface treatment; however, its bonding strength is hard to enhance or adjust [6-8]. In addition, the PMH interface prepared by ordinary processing methods often has a lot of defects, such as bubbles, looseness, poor fitting, thermal expansion coefficient mismatch, aging, and degumming [9], which have a great negative impact on its performance.

For the bond between two materials of metal and resin, their interfaces do not produce interfacial reaction layers similar to intermetallic compounds, and generally require introducing intermolecular bonding forces such as van der Waals or electrostatic forces to achieve bonding effects. To make the bonding strength of PMH meet the practical requirements, progress such as the enhancement of polymer basement and surface modifying of metal subtract has been made [10]. Guo *et al.* [11] modified the copper surface by anodizing and then treated with

Xi Liu, Ling Long, Hailong Wang, Qingchun Wang, Jing Qi, Jia Chen, Ji Liu: School of Automotive Engineering, Chengdu Aeronautic Polytechnic, Chengdu, 610100, China

Qingfeng Guo: School of Aeronautical Manufacturing Industry, Chengdu Aeronautic Polytechnic, Chengdu, 610100, China Yan Long: School of Basic Education, Chengdu Aeronautic Polytechnic, Chengdu, 610100, China

especially the packing materials of automobiles, electronic products, and furniture.

^{*} Corresponding author: Ying Li, School of Mechanical Engineering, Chengdu University, 2025 Chengluo Avenue, Chengdu, 610106, China, e-mail: liying@cdu.edu.cn

^{*} Corresponding author: Zuowan Zhou, Institute of Frontier Science and Technology, Southwest Jiaotong University, Chengdu, 610031, China, e-mail: zwzhou@swjtu.edu.cn

aqueous solution containing phosphate and sodium dihydrogen phosphate as corrosion solution to obtain a micronano structure on the copper. With optimized conditions, including voltage, treating time, and the phosphoric acid mass fraction, the copper surface is relatively smooth, and the porosity reaches 25.77%. In addition, introducing chemical interaction between polymer and metal is another way to enhance the bonding strength of PMH, such as the reaction between metallic silver and imidazole [12], the coupling effect between the silane coupling agent and stainless steel [13]. Above all, the interface structure is the key part that determines the mechanical strength of PMH, and most of the research works focus on the surface morphology of the metal substrate and the micro morphology of the bonding interface [14,15]. Moreover, processing methods include ultrasonic welding [16], lap welding [13], and radio frequency sputtering [17], etc. However, changing the processing method is troublesome and costly. On the contrary, changing the properties of the material itself is easy to achieve, and can greatly improve the interface bonding strength of the composites.

Most metal resin composite materials use aluminum or aluminum alloy as the metal matrix. And there have been abundant literature reports on the aluminum surface treatment process whose process and mechanism are very mature [15]. The preparation methods of aluminum surface nanostructures can be divided into chemical and physical methods. Chemical methods mainly include electrochemical etching and chemical etching, and physical methods mainly include mechanical processing methods such as laser etching [18], anodizing [19], and shot peening [20]. Among them, the anodizing is one of the most popular methods to generate pores on aluminum surface due to the stability process and result, and the bonding strength of the PMH fabricated with anodized aluminum is remarkably high, which makes the anodized aluminum widely used in industries. Even though, so far, there are only few studies on the influence of metal substrates with different surface morphologies on the bonding strength of aluminumbased PMH.

Therefore, in order to solve this problem, this article used electrochemical to treat Al alloy substrates with different anodizing conditions, and used NMT to prepare PMH. The results show that the anodizing voltage and time have substantial impact on the surface morphology of Al, which results in different bonding strength. By tuning the anodizing condition, PMH containing Al substrate anodized at 15 V for 6 h reaches 1,543 N of bonding strength. In addition, the interface structure and the chemical interaction between Al and polymer was studied, and the results indicate that polymer and metal form an

interpenetrated structure at the interface, and a chemical interaction exists between them. Both the physical structure and chemical interaction contributes to the high bonding strength of PMH.

2 Experimental

2.1 Materials

Al alloy plates was purchased from Taili metal factory. Before using, the Al plates were cut into $40~\text{mm} \times 10~\text{mm} \times 2~\text{mm}$ and polished by 80 Grit sandpaper to remove the oxides. Then, the plates were cleaned in acetone and ethanol that were purchased from Chengdu Kelong Chemical Co., Ltd. Polyphenylene Sulfide (PPS) was purchased from Da Han Chemical Company, which was dried at 140°C for 24~h to remove the water.

2.2 Surface treatment of Al plates and fabrication of PMH

The electrolyte contains $20 \text{ wt}\% \text{ H}_2\text{SO}_4$ and 80 wt% deionized water, and the Al plate was used as the anode, and the graphite sheet was used as the cathode. Anodizing was performed at 20°C under different voltages and stirring times. After anodizing, the Al plate was dried in an oven at 60°C for 20 min. Then, the plate was put into a pre-designed mold (Figure 1) and injection was performed. The Al cavity is filled by Al plate and the anodized area faces the injection cavity, and then, the polymer is injected into the injection cavity through injection port. Due to the high pressure and good fluidity of the polymer, it would be injected into the pores on the Al surface at the bonding area to form PMH. The mold temperature was set at 280°C , and the barrel temperature was set at 280°C . The injection time is 5 s and the compress time is 20 s.

2.3 Characterization

The morphology of the Al plates' surface nanostructures was investigated by field-emission scanning electron microscopy (FE-SEM, JEOL JSM-7800F, Japan). The operating voltage was 60.0 kV, the current was 100.0 mA, and the scanning range was 5–90°. When preparing SEM samples, a fine grinding machine (Leica EM TXP, Germany) was used

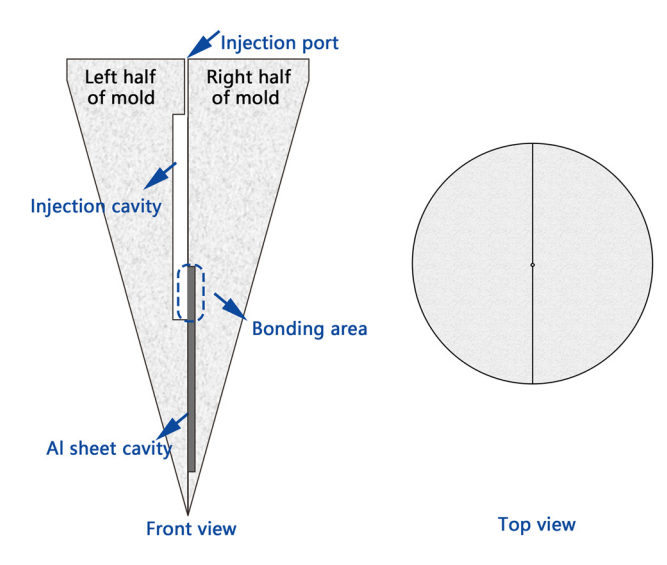


Figure 1: Schematic illustration of injection mold.

to finely grind the cross-section of PMH, so as to try to retain its original interface morphology, which is convenient for SEM observation. The reaction of the interface was carried out by Fourier Transform Infrared Spectroscopy (FT-IR) (PerkinElmer Spectrum 3, USA) with spectral resolution of 2 cm⁻¹ in a wavenumber region of 400–4,000 cm⁻¹ with ATR infrared spectroscopy mold. The thermodynamic behavior of the resin is characterized by Differential Scanning Calorimeter (DSC, 204 F1 Phoenix, Germany). The bonding strength between Al plates and PPS were tested by a microcomputercontrolled electronic universal testing machine (UTM4104X, Oberthur [Shandong] Testing Equipment Co., Ltd., China).

3 Results and discussion

3.1 Surface morphologies of Al alloy plates' surface

Based on the growth mechanism of anodized aluminum, voltage and anodizing duration play key roles in the pore diameter and depth [21,22]. The effects of voltage and time on the surface morphology of anodized aluminum were investigated. It can be seen from Figure 2a-c that the surface nanopore e increases as the anodizing time increases. At 15 V, the pores are in nano scale after 1.5 h of anodizing, while they increase to micro pores after 6 h of anodizing. The micro pores are favorable to fabricate PMH [23]. On elongation of the time, the pores collapse (Figure 2d). This is mainly because during the anodic oxidation process, gas will be deposited on the barrier layer on the metal surface, so the porous structure will continue to be produced [24]. However, when the time continues to increase, the electrons in the electrolyte will be transferred to the anode, breakdown of which will lead to some destruction of the pore structure [25]. In addition, as the anodic oxidation time increases, the thickness of the oxide layer will increase, and the oxide layer will be brittle, which will reduce the strength of the metal substrate [26]. Voltage has the same effect on pore size. As shown in Figure 2e and f, increasing voltage makes pore structure collapse rapidly. During the anodic oxidation process, with the increase in voltage, this energy balance

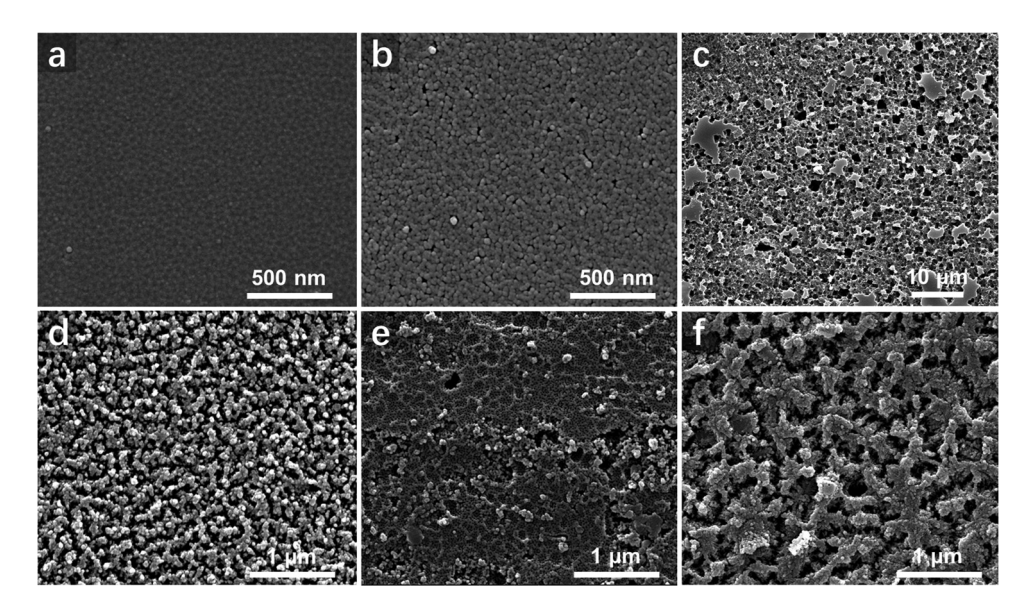


Figure 2: Surface morphologies of Al plates after anodizing. (a) The Al plates after cleaning, (b-d) Al plates anodized at 15 V for 1.5, 6, and 8 h, and (e and f) Al plates anodized for 6 h at 20 and 25 V, respectively.

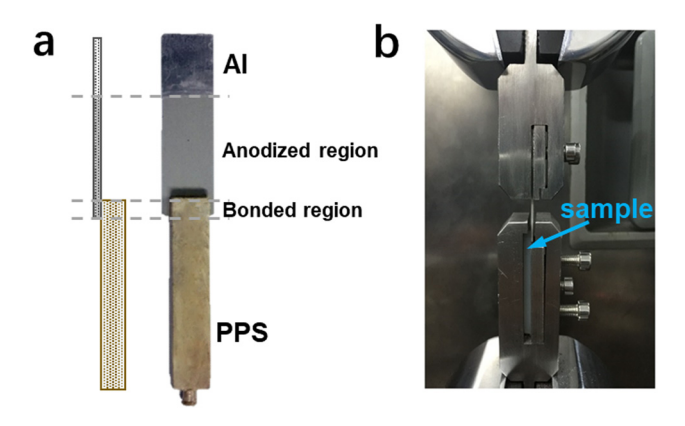


Figure 3: The digital photo of tensile testing: (a) the PMH sample and schematic illustration and (b) the test fixture.

will be destroyed, leading to the destruction of the pore structure.

3.2 Bonding strength of PMH

The Al alloy substrates prepared by the above preparation method and the PMH were prepared using a micro injection molding machine, and their bonding strength was tested by a tensile test. Figure 3a is the digital photo and schematic illustration of the PMH sample. In order to ensure the even force at both ends during the tensile testing, a gasket was placed on the bare metal end (Figure 3b). During the test, the thickness, width, and gauge length of the spline were not entered, and the maximum force was used to indicate the tensile strength.

The tensile test results are shown in Figure 4. It is clear that higher voltage and longer anodizing time are beneficial to increase the bonding strength of PMH. After polishing and cleaning, PPS is hard to be bonded with Al plate, and this phenomenon has been going on in PMH whose Al plate was anodized at 15 V for 1.5 and 4.0 h. With the further increase in anodizing time at 15 V, the bonding strength of PMH was significantly enhanced. A maximum bonding strength of 1,543 N was generated by the PMH anodized at 15 V for 6 h. However, when the anodizing time was further increased to 8 h, the bond strength decreased to 810 N. Based on the anodizing theories, the anodizing time positively relates to the pore depth, and which acts as the anchor to hitch resin in PMH [19,23,27]. Anodizing voltage also plays important role in pore structure on the metal surface. On increasing the voltage to 20 and 25 V, the pore collapsed, which results in decrease in bonding strength (Figure 4a). Figure 4b shows the different fracture modes of PMH, which indicates the effect of component material strength and interfacial structure on the bonding strength of PMH. For relatively smoother surface, the PPS is barely adhered on Al plate, and the weak bonding strength leads to complete separation of the metal and resin. For PMH with high bonding strength, it fractured on PPS body or the surface of Al plate. The proper pore structure allows great anchor structure of PMH and leads to high bonding strength. However, excessive anodizing makes the oxidation layer thicker that causes a peeled off oxide layer on Al plate during the tensile test.

3.3 Bonding mechanism analysis

In order to study the bonding mechanism between PPS and Al plates, first, the SEM characterization of the composite sample was performed. A series of fine grinding processes

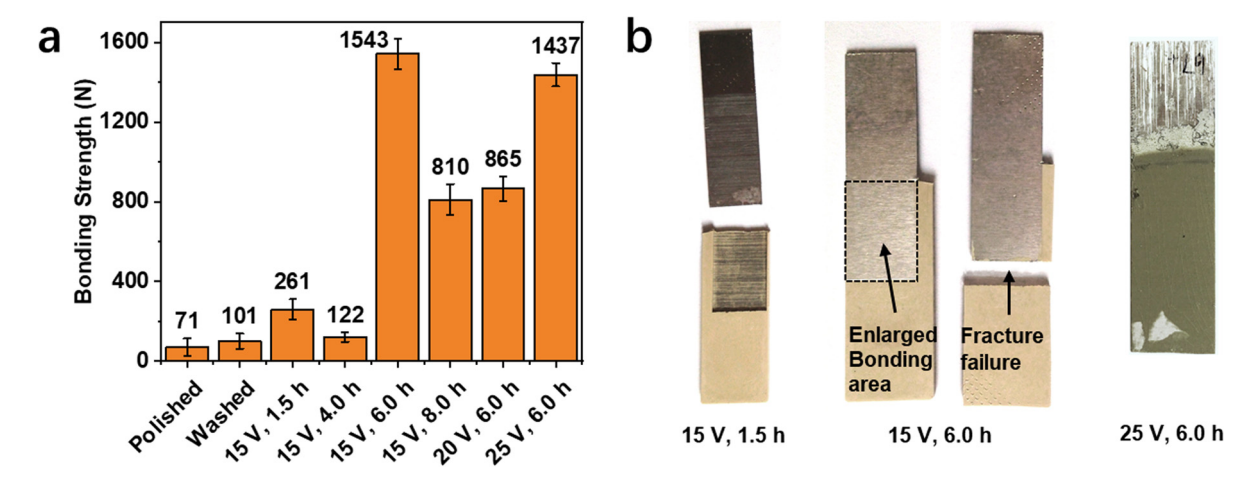


Figure 4: The tensile testing results: (a) the bonding strength results and (b) the PMH sample after tensile test.

were performed on the cross-section of PMH to obtain the cross-sectional morphology. As shown in Figure 5a, the boundary between Al plates and PPS in the PMH containing Al plate anodized at 15 V for 6 h is quite clear, and the PPS and Al plate are tightly bonded due to no obvious gap has been found in this boundary. While there exists a gap between PPS and Al plates in the PMH containing Al anodized at 20 V for 6 h (Figure 5b), which implies that the difference of surface structure on Al is dominant in the bonding strength. As mentioned previously, the pores on Al plate obtained by 6 h of anodizing at 15 V are in macro size, and the pores on Al plate obtained by 6 h of anodizing at 20 V collapses and are mostly in nano size. During injection, the relatively larger pores allow the polymer to fill the cavity more fully, while the smaller pores reject the PPS and gaps would be generated between PPS and Al plate due to different thermal expansion rates. The Al substrate of PMH is dissolved by alkaline to expose the surface morphology of PPS facing the interface. As shown in Figure 5c and d, the residue polymer displays a surface with bulges, which is the same as the pores on the anodized Al plate surface (Figure 2c), which indicates that the polymer has been injected into the pores on Al plates' surface. There is a transition layer between Al and PPS where the metal matrix and the polymer PPS interpenetrate into each other. This transition layer connects Al plate and PPS closely, and the interface between the resin and the metal almost disappears. Comparing the interface of PMH containing Al plate anodized at 15 V for

6 h, the PMH containing Al plate anodized at 20 V shows no transition layer (Figure 5b), which explains its lower bonding strength. Figure 5e is the SEM image of an interpenetrating structure constructed by the anchor PPS and the bolt pores on Al plate's surface, which further proves that the PPS has been injected into the pores on Al plate by NMT. This structure is also confirmed by the element analysis, in which the Al exists on the PPS region and S shows on the Al region (Figure 5f). The formation of anchor and bolt structure is beneficial for bonding PPS and Al.

Attenuated total reflection (ATR) infrared spectroscopy characterization method is used to analyze the chemical interaction between metal and resin. The ATR is an effective means to characterize the interface of PMH. Unlike ordinary transmission, ATR does not require incident light to pass through the sample, and can be used to detect opaque solid samples [28-30]. Characterizing the instantaneous vibration of chemical bonds to determine the existence and function of chemical bonds can facilitate the study of PMH interface interactions. Figure 6a is the ATR spectrum of PMH and PPS with a resolution of 2 cm⁻¹. In the spectrum, 1,569, 1,472, and 1,387 cm⁻¹ are the stretching vibration peaks of the aromatic ring, 1,008 cm⁻¹ is the plane deformation vibration peak of the aromatic ring, and 806 cm⁻¹ is the out-of-plane deformation vibration peak of C-H bond of the aromatic ring [31]. In the ATR spectrum of PPS bulk, the absorption peak at 1,093 cm⁻¹ is the stretching vibration absorption peak of

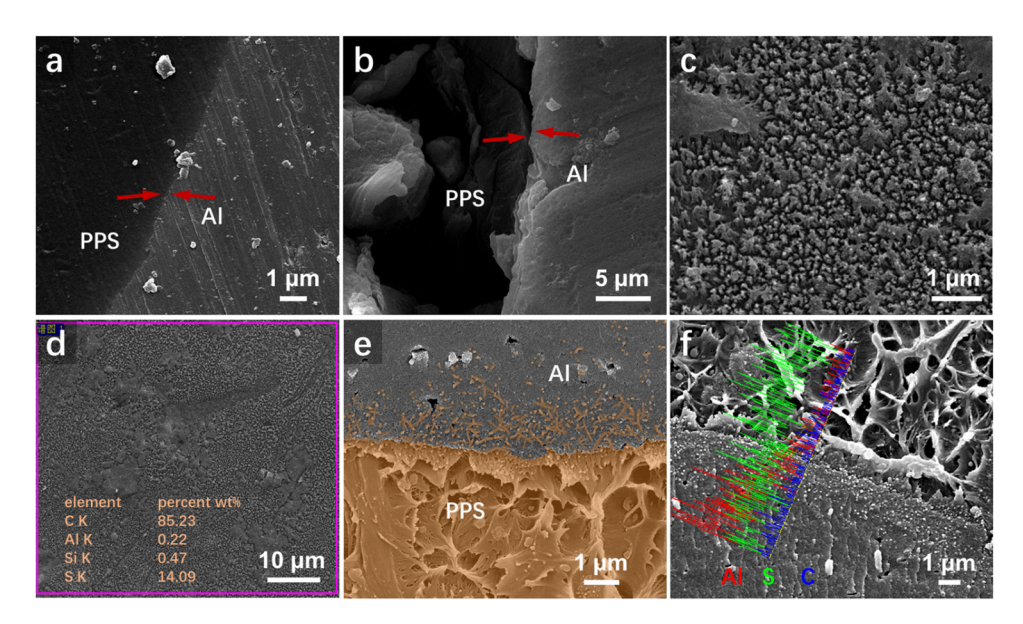


Figure 5: The SEM images of PMH interface. The cross-section image of PPS/Al boundary in which the Al plate was anodized for 6 h at 15 V (a) and 20 V (b). (c) The exposed PPS surface of PMH after dissolving the Al matrix, (d) the element mapping of (c), (e) the front image showing the anchor and bolt structure that constructed by PPA and Al, where the PPS was rendered yellow, and (f) the element distribution around boundary.

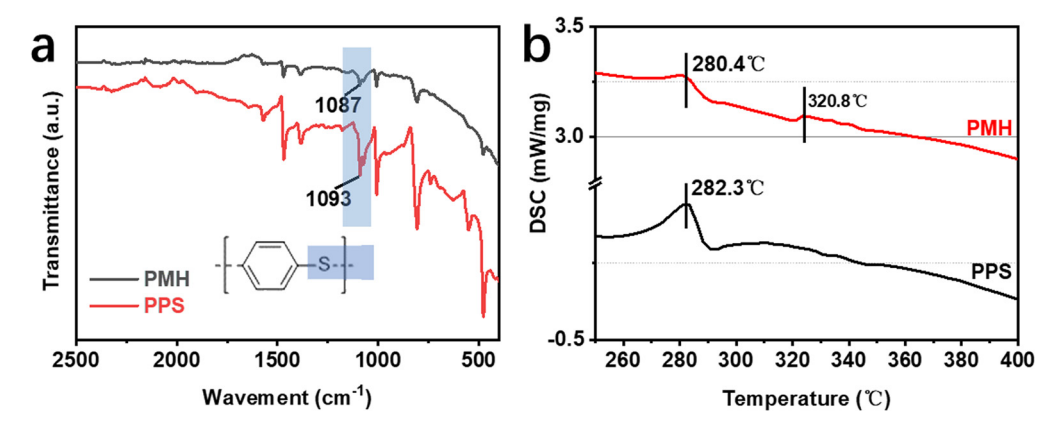


Figure 6: Structural analysis of PMH: (a) the ATR spectrum and (b) the DSC curves of PPA and PMH.

C-S, and the frequency corresponding to 1,093 cm⁻¹ belongs to the C-S fingerprint frequency [32]. In the ATR spectrum of PMH, the stretching vibration absorption peak wave number of C-S shifted to 1,087 cm⁻¹, indicating that there is an interaction between PPS and Al in PMH, which leads to a decrease in the bond energy of the C-S bond [33]. PPS is a semi-crystalline resin [34], which can easily contact with alumina with nanopores on the surface. From a spatial point of view, the gyration radius of the PPS is less than 100 nm, and the alumina nanopore diameter is larger than 100 nm. Some scholars believe that the pore diameter of the nanopore affects the local polymer chains [35–37]. The higher the bulk density of the polymer chain, the greater the resistance to the movement, which may cause the shift of the infrared absorption peak [38]. From the structural point of view, C-S is a polar bond, and S atoms are chemically active, which may chemically interact with the metal surface and cause the shift of infrared absorption peaks. In addition, due to restrictions or other factors, the crystallinity of PPS may decrease, and the polymer segments move more freely, resulting in the shift of infrared absorption peaks [39].

DSC was performed to study the thermodynamic behavior of bulk PPS and the PPS in the PMH, and the results are shown in Figure 6b. It is found that PPS in the composite is different from its own melting point, and there exists two melting peaks. The reason for the bimodal melting of polymers is the existence of different kinds of crystallization or melting recrystallization, which indicates that the crystallization behavior of PPS in composite materials is affected. When the polymer is confined to nanopores, the radial distribution density of the melt is uneven, resulting in different chain packing density near the pore wall, and the higher the density, the more difficult the movement of molecular chains [40,41]. As the distance from the hole wall increases, the chain density decreases, and the movement of the molecular chain gradually approaches the body [42]. Theoretically, the crystallization of PPS has influence on the bonding strength of PMH because of the effects on PPS's mechanical strength, and generally, higher crystallization degree results in higher mechanical strength of polymer [43]. Polymer and metal interpenetrate into each other at the interface to form an anchor and bolt structure, in which the polymer acts as the

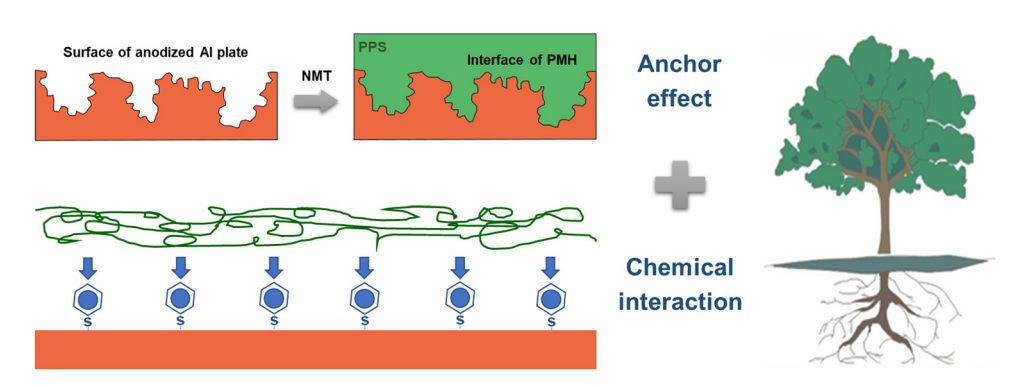


Figure 7: Schematic illustration of the bonding mechanism of PMH.

anchor whose mechanical strength determines the deformation behavior under stress/strain.

Based on the above study, the bonding mechanism of PMH is concluded and illustrated in Figure 7. First, the pores on the metal surface offer the anchor and PPS acts as the bolt to form a physically interpenetrated structure that was proved by sufficient morphological and structural analysis. Here the pore size should be controlled carefully. The interpenetrated structure is like the roots buried in the ground that makes the tree stand steady on the land. Second, the anodized Al surface chemically interacts with PPS, which is confirmed by ATR analysis. Both physical and chemical interactions attribute the high bonding strength of PMH containing Al plate and PPS by NMT.

4 Conclusion

In this work, the preparation and bonding mechanism of metal resin composite has been studied. The PMH was successfully fabricated by NMT, and the bonding strength between metal and polymer shows dependence on the pore structure of metal surface, which could be controlled by changing the anodizing voltage and time. The PMH in which the Al plate was anodized at 15 V for 6 h achieves the best bonding strength of 1,543 N. The morphological analysis reveals that there forms an anchor and bolt structure in the interface of PPS and Al plate, which bonds the polymer and metal tightly. In addition, the chemical interaction between PPS and Al were confirmed by ATR, which indicates that both physical and chemical effects contribute to the bonding strength of PMH. This study enriches the research on the bonding mechanism of PMH, and the excellent PMH obtained in this paper is potential to be used as alternative to pure metal packaging components in automobiles and mobile phones.

Funding information: This work was financially supported by the Research Startup Foundation of Chengdu University (No. 30-2081921081), 2021 Natural Scientific Research Project of Chengdu Aeronautic Polytechnic (No. 06211012), and the Open Project of Sichuan International Joint Research Center for Robotics and Intelligent Systems (No. JQZN2021-004). In addition, we would like to thank the Institute of Advanced Study of Chengdu University for supporting the relative measurements.

Author contributions: All authors have accepted responsibility for the entire content of this manuscript and approved its submission.

Conflict of interest: The authors state no conflict of interest.

References

- Yang B, Zhang Y, Xuan FZ, Xiao B, He L, Gao Y. Improved adhesion between Nickel-Titanium SMA and polymer matrix via acid treatment and nano-silica particles coating. Adv Compos Mater. 2017;27(3):331-48.
- Wang F, Wang Q, Huang H, Cheng Y, Wang L, Ai S, et al. Effects of laser paint stripping on oxide film damage of 2024 aluminium alloy aircraft skin. Opt Exp. 2021;29(22):35516.
- Annerfors CO, Petersson S. Nano molding technology on cosmetic aluminum parts in mobile phones-an experimental study. Sweden: Lund University; 2007.
- Liu D, Zhou F, Li H, Xin Y, Yi Z. Study on the interfacial interactions and adhesion behaviors of various polymermetal interfaces in nano molding. Polym Eng Sci. 2020;61(1):95-106.
- Zhang N, Byrne CJ, Browne DJ, Gilchrist MD. Towards nanoinjection molding. Mater Today. 2012;15(5):216-21.
- Li Y, Mei Y, Wang Y, Meng F, Zhou Z. The State-of-Art of nanomolding technique applying to the production of metal/ polymer composites. Mater Rev. 2018;32(7):2295-303.
- Liu D, Zhou F, Zhou H. The Polymer-metal interactive behavior in polyphenylene sulfide/aluminium hetero interface in nano injection molding. Compos Interface. 2019;27(3):277-88.
- Liu Y, Jia M, Song C, Lu S, Wang H, Zhang G, et al. Enhancing ultra-early strength of sulphoaluminate cement-based materials by incorporating graphene oxide. Nanotechnol Rev. 2020;9(1):17-27.
- Lambiase F, Scipioni SI, Lee CJ, Ko DC, Liu F. A state-of-the-art review on advanced joining processes for metal-composite and metal-polymer hybrid structures. Materials. 2021;14(8):1890.
- [10] Fu H, Xu H, Liu Y, Yang Z, Kormakov S, Wu D, et al. Overview of injection molding technology for processing polymers and their composites. ES Mater Manuf. 2020;8:3-23.
- Guo RS, Hu GH, Jian R, Yuan LW. Copper surface treatment in [11] metal-polymer direct molding technology. J Shanghai Jiao Tong Univ (Sci). 2021;55(1):96-102.
- Kakuta K, Urapepon S, Miyagawa Y, Ogura H, Suchatlampong C, Rittapai A. Development of metal-resin composite restorative material. Part 4. Flexural strength and flexural modulus of metal-resin composite using Ag-In alloy particles as filler. Dent Mater J. 2002;21(2):181-90.
- [13] Liu FC, Liao J, Nakata K. Joining of metal to plastic using friction lap welding. Mater Des. 2014;54:236-44.
- Kang Z, Shi Z, Lei Y, Xie Q, Zhang J. Effect of the surface morphology on the bonding performance of metal/composite hybrid structures. Int J Adhes Adhes. 2021;111:102944.
- Goushegir SM, dos Santos JF, Amancio FST. Influence of aluminum surface pre-treatments on the bonding mechanisms and mechanical performance of metal-composite single-lap joints. Weld World. 2017;61(6):1099-115.
- [16] Elsheikh AH, Abd Elaziz M, Vendan A. Modeling ultrasonic welding of polymers using an optimized artificial intelligence

- model using a gradient-based optimizer. Weld World. 2021;66(1):27-44.
- [17] Hwang JD, Chiou YJ. Thermal treatment for enhancing performance of NiO/Ag/NiO transparent conducting electrode fabricated via magnetron radio-frequency sputtering. J Alloy Compd. 2021;883:160892.
- [18] Huang LJ, Zhao L, Li BJ, Zhang Y, Wang YI, Wang YY, et al. Improving optical and electrical performances of aluminum-doped zinc oxide thin films with laser-etched grating structures. Ceram Int. 2021;47(6):7994–8003.
- [19] Chen X, Li Y, Wang Y, Song D, Zhou Z, Hui D. An approach to effectively improve the interfacial bonding of nano-perfused composites by *in situ* growth of CNTs. Nanotechnol Rev. 2021:10(1):282-91.
- [20] Chang YP, Chu LM, Liu CT, Wang JC, Chen KW. Effects of shot peening on the tribological properties of aluminum alloys with T6 treatment. J Phys Conf Ser. 2021;2020(1):012013.
- [21] Kim D, Jung S, Yoon C. Evaluation of airborne total suspended particulates and heavy metals in anodizing and electroplating surface treatment process. Sci Rep. 2021;11(1):22537.
- [22] Iwai M, Kikuchi T, Suzuki RO. Self-ordered nanospike porous alumina fabricated under a new regime by an anodizing process in alkaline media. Sci Rep. 2021;11(1):7240.
- [23] Kimura F, Kadoya S, Kajihara Y. Effects of molding conditions on injection molded direct joining using a metal with nanostructured surface. Precis Eng. 2016;45:203–8.
- [24] Thompson GE, Xu Y, Skeldon P, Shimizu K, Han SH, Wood GC. Anodic oxidation of aluminium. Philos Mag B. 2006;55(6):651–67.
- [25] Schwirn K, Lee W, Hillebrand R, Steinhart M, Nielsch K, Gösele U. Self-ordered anodic aluminum oxide formed by H₂SO₄ hard anodization. ACS Nano. 2008;2(2):302-10.
- [26] Tian W, Li J, Liu Y, Ali R, Guo Y, Deng L, et al. Atomic-scale layer-by-layer deposition of Fesial@Zno@Al₂O₃ hybrid with threshold anti-corrosion and ultra-high microwave absorption properties in low-frequency bands. Nanomicro Lett. 2021;13(1):161.
- [27] Power AC, Gorey B, Chandra S, Chapman J. Carbon nanomaterials and their application to electrochemical sensors: a review. Nanotechnol Rev. 2018;7(1):19-41.
- [28] Kazarian SG, Chan KL. Micro- and macro-attenuated total reflection Fourier transform infrared spectroscopic imaging. Plenary lecture at the 5th international conference on advanced vibrational spectroscopy, 2009, Melbourne, Australia. Appl Spectrosc. 2010;64(5):135A-52A.
- [29] Lancefield CS, Constant S, de Peinder P, Bruijnincx PCA. Linkage abundance and molecular weight characteristics of technical lignins by attenuated total reflection-FTIR spectroscopy combined with multivariate analysis. ChemSusChem. 2019;12(6):1139–46.

- [30] Chiarello GL, Ferri D, Selli E. *In situ* attenuated total reflection infrared spectroscopy study of the photocatalytic steam reforming of methanol on Pt/TiO₂. Appl Surf Sci. 2018;450:146–54.
- [31] Ildiz GO, Tabanez AM, Nunes A, Roque JPL, Justino LLG, Ramos ML, et al. Molecular structure, spectroscopy and photochemistry of alprazolam. J Mol Struct. 2022;1247:131295.
- [32] Ribeiro AS, Costa SM, Ferreira DP, Calhelha RC, Barros L, Stojković D, et al. Chitosan/nanocellulose electrospun fibers with enhanced antibacterial and antifungal activity for wound dressing applications. React Funct Polym. 2021;159:104808.
- [33] Michell RM, Muller AJ. Confined crystallization of polymeric materials. Prog Polym Sci. 2016;54–55:183–213.
- [34] Golzar M, Sinke J, Abouhamzeh M. Novel thermomechanical characterization for shrinkage evolution of unidirectional semi-crystalline thermoplastic prepregs (Pps/Cf) in melt, rubbery and glassy states. Compos Part A Appl S. 2022;156:106879.
- [35] Xue J, Xu Y, Jin Z. Interfacial interaction in anodic aluminum oxide templates modifies morphology, surface area, and crystallization of polyamide-6 nanofibers. Langmuir. 2016;32(9):2259–66.
- [36] Zhang L, Wei Q, An J, Ma L, Zhou K, Ye W, et al. Construction of 3D interconnected diamond networks in Al-matrix composite for high-efficiency thermal management. Chem Eng J. 2020;380:122551.
- [37] Jimenez AM, Altorbaq AS, Müller AJ, Kumar SK. Polymer crystallization under confinement by well-dispersed nanoparticles. Macromolecules. 2020;53(22):10256-66.
- [38] Sha Y, Qi D, Luo S, Sun X, Wang X, Xue G, et al. Synthesis of site-specific dye-labeled polymer via atom transfer radical polymerization (ATRP) for quantitative characterization of the well-defined interchain distance. Macromol Rapid Commun. 2017;38(2):1600568.
- [39] Luo S, Li N, Zhang S, Zhang C, Qu T, Ocheje MU, et al. Observation of stepwise ultrafast crystallization kinetics of donor-acceptor conjugated polymers and correlation with field effect mobility. Chem Mater. 2021;33(5):1637-47.
- [40] Meldrum FC, O'Shaughnessy C. Crystallization in confinement. Adv Mater. 2020;32(31):e2001068.
- [41] Lei M, Chen Z, Lu H, Yu K. Recent progress in shape memory polymer composites: methods, properties, applications and prospects. Nanotechnol Rev. 2019;8(1):327–51.
- [42] Staub MC, Li CY. Confined and directed polymer crystallization at curved liquid/liquid interface. Macromol Chem Phys. 2017;219(3):1700455.
- [43] Wach RA, Wolszczak P, Adamus WA. Enhancement of mechanical properties of FDM-PLA parts via thermal annealing. Macromol Mater Eng. 2018;303(9):1800169.